Towards Efficient Hyperspectral Object Detection and Classification using Thermal Optimization Algorithm with Deep Learning

Noor Edin Rabeh
Baghdad University, College of Science, Baghdad, Iraq
Edinnoori45@gmail.com

Abstract

Object detection in remote sensing images (RSI) is a main procedure where the purpose is to automatically recognize and categorize certain objects or features from large-scale, remotely developed images like aerial imagery or satellite. This task role a vital play in extracting appreciated data from massive geographical regions, contributing to various applications under several domains namely environmental monitoring, urban planning, agriculture, and disaster management. Recent developments in deep learning (DL) technologies have significantly enhanced the accuracy and efficacy of object detection systems for RS, enabling more precise and automated analysis of various landscapes and facilitating informed decision-making. DL approaches namely convolutional neural networks (CNNs) are exposed to remarkable abilities in learning intricate patterns and features from difficult spatial data, resulting in enhanced accuracy and effectiveness. In this article, we present a Towards Efficient Hyperspectral Object Detection and Classification using Thermal Optimization Algorithm with Deep Learning (HODC-TOADL) system. The objective of HODC-TOADL algorithm is to identify and categorize distinct types of objects that exist in the RSI. In the HODC-TOADL method, an improved Dense Net model is applied to learn the distinct features of the input RSI. Besides, the TOA has been deployed to boost the hyper parameter choice of the Dense Net method. Furthermore, the classification of objects can be carried out by employing of adaptive neurofuzzy inference system (ANFIS). The experimental evaluation of the HODC-TOADL algorithm can be studied on benchmark databases. The experimental values stated that the HODC-TOADL algorithm reaches effective classification performance compared to recent DL models.

Keywords: Object Detection; Remote Sensing Images; Deep Learning; Thermal Optimization Algorithm; ANFIS

1. Introduction

In the present scenario, the remote sensing images (RSI) application database has become more significant in our everyday actions. Object recognition and image identification from the diagnosis of multi-temporal higher resolution RSI has become vastly beneficial in real uses such as natural disasters, environmental monitoring, dangerous actions avoidance, and global biodiversity analysis [1]. Diagnosis of RSI is highly challenging owing to the difficult nature of the imageries. The growth of reliable methods for the RSI analysis is extremely significant. The physical classification and recognition of objects and images from RSI is difficult and expensive [2]. There are numerous methods generated to identify objects and categorize images from RSI. Currently, there are extensive tries to integrate machine learning (ML) models into the growth of methods for the diagnosis and identification of RSI in object recognition [3]. Massive amounts of RSI data are gained from imaging optical sensors on false satellites of Earth and aerial platforms; such techniques have the benefits of being genuine and available in real time [4]. As per diverse imaging spectral sorts, the data can be categorized as infrared, ultraviolet visible, hyperspectral, multi-spectral, or SAR images. These imageries make different assistances to the Earth Observation System, inspiring our understanding of the atmosphere and enabling people's actions [5]. Currently, there is a rapid growth of RSI platforms and sensors, the point that the quality and quantity of remote sensing data are enhancing a novel issue, i.e., how to efficiently utilize present data and increase their value of application [6].

DOI: https://doi.org/10.54216/IJAACI.060201
Received: November 12, 2023 Revised: January 29, 2024 Accepted: June 23, 2024

Therefore, object recognition utilizing RSI, as a simple image analysis application, is getting more attention from researchers. The task of RSI object recognition is extremely challenging and has wider application predictions like face recognition, automatic driving, medical detection, pedestrian detection, and so on. Simultaneously, object recognition is mainly employed for image description, image segmentation, action recognition, object tracking, and other more difficult computer vision (CV) challenges [7]. Feature extraction, pre-processing, and object classification are normally the 3 procedures of traditional RSI object recognition models. Deep learning (DL)-based object detection models have gradually developed as CV and DV have advanced, which can resolve the restrictions of classical models and have important innovations in RSI object detection [8]. When equated to the conventional model based on physical features, the object detection technique based on DL has major benefits. Traditional approaches normally need physical designs of feature extractions, and the result is restricted below difficult acts and extremely variable states [9]. However, object recognition models dependent upon DL can learn feature representations straight from the original image through endwise training without trusting hand-designed feature extractions [10]. The Convolutional Neural Network (CNN) DL system can remove rich feature data from imageries and take semantic data at dissimilar stages, therefore enhancing the accuracy and generalization capability of object recognition.

This article presents a Towards Efficient Hyperspectral Object Detection and Classification using a Thermal Optimization Algorithm with DL (HODC-TOADL) approach. The objective of HODC-TOADL technique is to identify and classify distinct kinds of objects existing in the RSI. In the HODC-TOADL technique, an improved Dense Net model is applied to learn the distinct features of the input RSI. Besides, the TOA has been deployed for boost parameter choice of the improved Dense Net technique. Furthermore, the classification of objects can be carried out by the employ of an adaptive neuro-fuzzy inference system (ANFIS) system. The experimental values of the HODC-TOADL method has been studied on benchmark databases.

2. Literature Review

Zhang et al. [11] developed a tree-shaped multi-objective evolutionary CNN (TMOE-CNN) for HSI classification. A multi-branch super network structure was developed that resembles a tree as the basic model for the network blocks. In [12], an effective HSI salient object detection technique was developed by anomaly recognition by integrating DL auto-encoders (AE) with one-class SVM. This developed technique primarily utilizes deep-AE to design the context of an input HSI image with respect to spectral reconstruction residuals of the AE followed by identifying the salient objects in the image via one class SVM-based anomaly detection. Mahgoub et al. [13] introduced a Hyperspectral Object Detection employing Bio-inspired Jellyfish Search Optimizer with DL (HSOD-JSODL) method that utilizes an EfficientDet object detector. EfficientDet was a recently developed object detector that incorporates effectiveness through a compound scaling technique and effectual network. Moreover, the method employs a DBN algorithm for the classification of identified objects. Besides, the JSO method was implemented as a hyper parameter optimizer.

In [14], a dual-channel DL feature fusion model (DLFM) has been presented. The DLFM technique removes spectral features employing a 1-D convolution component and spatial image features from the RGB image employing a 2-D convolutional component. These features were combined by employing a feature adaptive fusion method. SVM, 1D-CNN, 2D-2DCNN, and DLFM have been made correspondingly. Alajmi et al. [15] presented a dandelion optimizer with DTL-based crop type detection and classification (DODTL-CTDC) algorithm. This method employs the Exception for the extractor. Moreover, the hyper parameter choice of the Exception architecture arises by employing the DO technique. Furthermore, the CAE method was implemented in the classification. Moreover, an AOA could be utilized for optimum hyper parameter selection. In [16], a CNN technique-based salient object detection algorithm was developed by employing HSI for the usage of spatial and spectral data concurrently. The developed technique integrates an extended morphological profile (EMP) method and then a CNN for employing the data from adjacent pixels and higher-level features concurrently.

Zhao et al. [17] developed an HSI classification technique dependent upon a channel perception mechanism and a hybrid deformed convolution network (CPM-HDCN). Particularly, a CPM dependent upon regression and ranking loss functions was developed. Next, a foreground-background image for every type instance was formed. Lastly, an HDCN was employed for classifying the HSI and then, channel aware feature extraction. Islam et al. [18] projected an architecture that integrates reduce size and re-sampling as pre-processing stages for a DL method. This approach utilizes an innovative subgroup-based dimensionality reduction method for extraction. Furthermore, the data was resampled to accomplish the class balance through each type. The decreased and balanced data have been further processed by employing a hybrid CNN method that integrates 3D and 2D learning blocks for extracting spectral-spatial features and accomplishing reasonable classifier accuracy.

DOI: https://doi.org/10.54216/IJAACI.060201
Received: November 12, 2023 Revised: January 29, 2024 Accepted: June 23, 2024

3. The Proposed Method

In this study, we design an efficient HODC-TOADL methodology. The HODC-TOADL approach aims to identify and categorize distinct kinds of objects that exist in the RSI. To attain this, the HODC-TOADL technique comprises three distinct processes such as Dense Net-based feature extractor, TOA-based parameter tuning, and ANFIS-based classification method. Fig. 1 portrays the working flow of the HODC-TOADL method.

3.1. Dense Net-based Feature Extraction

Initially, the HODC-TOADL technique undergoes an improved Dense Net model applied for learning the distinct features of the input RSI. The Dense Net is a dense CNN developed. The foremost Dense Net structure is the centre dense block (DB) [19]. The internal dense module contains of ReLU activation function, batch normalization (BN), and $1x1$ and $3x3$ convolutional layers (Conv). Every neuron is just linked to its preceding neuron and also creates links with the back neuron; a DB has L neurons, they are $Lx(L+1)/2$ connections, and the first layer output is

$$X_l = H_l([x_0, x_1, \dots, x_{l-1}]) \quad (1)$$

Here, H_l signifies the Conv layer operation l, and x_l denotes the output. Normally to prevent difficult computations, a module of bottleneck, which is a $1x1$ Conv layer is inserted into the DB to decrease the feature counts. Nearby DB has been linked over transition layer to decrease the complete parameter number of the network and enhance computation ability. The transition layers contain of Conv layer and an $2x2$ average pooling layer.

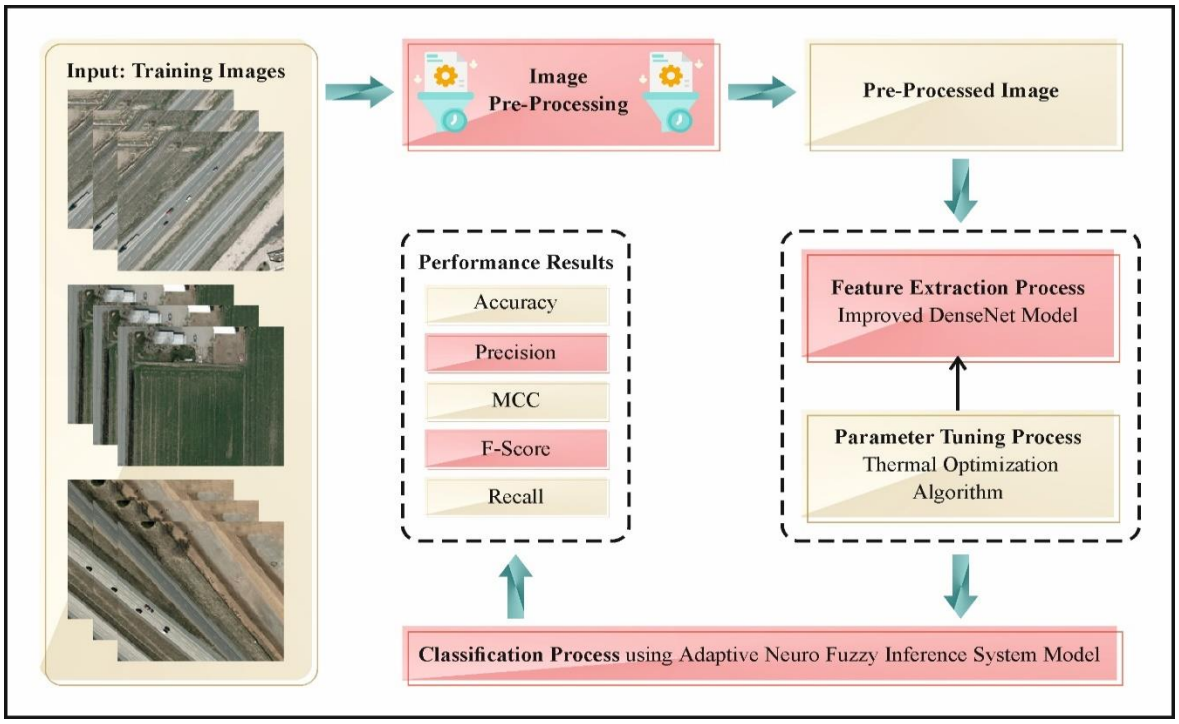

Fig. 1. Workflow of HODC-TOADL technique

Employing the network of DenseNet for classification, while the gradient disappearance issue has been improved to a definite amount thus the connections among any dual layers is an equivalent resultant fusion. For every layer input, the upper layer output of the chief road must be utilized as a significant processing objective of the low layer input. The united output of the preceding layer must decrease the ratio consequently but the deeper layer can employ the feature removed from a few previous layers openly. The transition layers will output a huge amount of terminated features, which result in lower operation of the preceding output feature by later DB. The SE is inserted into the structure of DenseNet. Next, the weight adaptive model has been implemented, and then the weight of every channel has been assigned by employing the connection of the feature channel, to allow the NNs to absorb significant feature data and decrease the effect of redundant feature.

DOI: https://doi.org/10.54216/IJAACI.060201
Received: November 12, 2023 Revised: January 29, 2024 Accepted: June 23, 2024

The SE mostly contains the simple structure of the global pooling, binary activation function, and FC layer. The compression process employs a pooling layer in order to compact the feature map of dimension $CxHxW$ (W is the width, H is the height and C denotes the feature channel counts) under the $Cx1x1$ feature, thus decreasing the number of parameters. Furthermore, it will not modify the entire channel size. When the dimension is $CxHxW$, then the input is set as $U = [u_1, u_2, \dots, u_c]$, the mapping connection of the compression process as:

$$Zc = Psq(u_c) = \frac{1}{H \times W} \sum_{i=1}^{H} \sum_{j=1}^{W} u_c\,(i,j) \tag{2}$$

Whereas $c \in C$, Zc signifies the overall data of $the\ c$ feature map, and Fsq denotes the process of squeeze. The process of excitation is comprised of an FC layer and the activation function of sigmoid. The FC layer incorporates the entire input normal data, and the sigmoid map the input in the range [0 and 1].

$$s = Fex(Z,W) = \sigma\big(g(Z,W)\big) = \sigma\big(W_2 \cdot \delta(W_1 \cdot Z)\big) \tag{3}$$

Here, δ refers to the ReLU, W_1, and W_2 refer to the parameters of weight, Fex denotes the excitation operation and σ specifies the sigmoid function. Lastly, the model executes the process of scale, increases the weight feature learned by SE, and merges the weight with the new feature. This delivers the merged input feature as an input, decreasing feature redundancy and enhancing the performance of the network as an outcome.

3.2. Hyper parameter tuning using TOA

In this study, the TOA has been deployed for optimal parameter choice of the improved Dense Net approach. The model of optimizer and the relationship between Newton's law of cooling and optimizer [20]. Normally, an optimizer has all models which are employed to discover the finest solutions for issues of optimization. Many techniques of optimizer are presented for this objective. Traditional models provide accurate outcomes for the issues of optimizer, but currently by enhance the difficulty of these issues. The capability to resolve the issues with these procedures is declining. Meta-heuristics are intellectual systems that are employed in order to discover the optimum solution and solve the aforementioned problems. Meta-heuristic models are calculation optimizers that have results to exit the local optimizer and are appropriate for an extensive sort of issue. Metaheuristic techniques are a motivation of numerous phenomena, animal behaviours, and backgrounds to human cultures and utilize these beginnings to pretend a model for resolving the optimizer issue. Many types of meta-heuristic models are projected currently namely elephant herding optimization, Thermal Exchange Optimizer (TEO), world cup optimizer, biogeography-based optimization, equilibrium optimizer, and ant lion optimizer (ALO).

Here, an improved intention of the TEO algorithm is mainly offered to deliver more capability in terms of consistency and accuracy. It is a motivation of the temperature objects' performance and their location that switched among warm and cold parts in order to specify the upgraded locations. In this optimizer, the individual has been divided into dual portions. One part is the candidate which is measured as a cooling substance, and the other part is reflected as the environment. Then, the contrary procedure is prepared.

The algorithm starts with a pre-defined amount of randomly generated individuals as the early results are as below:

$$T_j^0 = \underline{T} + \theta \times \left(\overline{T} - \underline{T}\right), j = 1,2,n, \tag{4}$$

Here, T_j^0 indicates the initial population, θ implies the random size from the range of 0 and 1, $\overline{and\ T}$ and $\underline{T}$ denote the maximal and minimal limitations, respectively.

Afterward attaining the cost value of the produced candidate, T amount of the finest cost individual places is kept as Thermal Memory (TM) to deliver greater efficacy with low difficulty to the system. Then, the TM individual is united to individuals and the equivalent amount of worse candidates is captured.

T_1 defines the object of environment for $T_{(n/2)+1}$, and inversely. If the object is lesser than ζ, then the temperature substitutes steadily. ζ has been expressed below:

$$\zeta = \frac{Cos(object)}{Cos(worst\ object)}. \tag{5}$$

DOI: https://doi.org/10.54216/IJAACI.060201
Received: November 12, 2023 Revised: January 29, 2024 Accepted: June 23, 2024

Time is an additional word in the model of the optimizer which is linked to the iteration count. It is attained by below mentioned expression:

$$t = \frac{iteration}{\text{Max.}\, iteration} \tag{6}$$

To increase the global search, the environmental temperature change is measured which is expressed below:

$$T_i^e = \left(1 - (\alpha_1 + \alpha_2 \times (1-t) \times \delta)\right) \times T_i^{\mathcal{R}}, \tag{7}$$

Here, δ defines a randomly generated number between 0 and 1, $T_i^{\mathcal{R}}$ denotes the previous object temperature adapted by T_i^e, α_1 and α_2 denote the control variables, correspondingly.

Lastly, the novel location for the object temperature has been attained as:

$$T_i^N = T_i^e + \left(T_i^{o1d} - T_i^e\right)\exp\left(-\zeta t\right). \tag{8}$$

Also, this algorithm describes whether a module variations in the cooling object or not. This is inspired by Pr. The Pr covers a few individuals that are equated with $R(i)$ that is a randomly produced value from the interval of zero and one. If $R(i)$ is lesser than Pr, then 1D of the i^{th} candidate is arbitrarily selected and the size is re-formulated as:

$$T_{i,j} = \underline{T_j} + \delta\left(\overline{T_j} - \underline{T_j}\right)\exp(-\zeta t), \tag{9}$$

Here, $\underline{T_j}$ and $\overline{T_j}$ denote the low and high limitations of the parameter number j, correspondingly. $T_{i,j}$ defines the variable number j. When the stopping criteria are attained, then the procedure is ended.

The TOA progresses a FF for attaining an enhanced classifier solution. It describes a positive integer to suggest the optimum solution for candidate outcomes. Now, the minimalized of the classifier error values can be supposed that FF is defined in Eq. (10).

$$fitness(x_i) = ClassifierErrorRate(x_i)$$
$$= \frac{No.of\ misclassified\ instances}{Total\ no.of\ instances} * 100 \tag{10}$$

3.3. ANFIS-based Classification Process

Eventually, the classification of objects can be carried out by the use of the ANFIS technique. The architecture of ANFIS proves that it includes NNs and fuzzy logic (FL) through 5 layers [21]. L. Zadeh abstracted FL and fuzzy inference systems (FIS) during the year 1965. Its objective is to overcome the complexity that occurs while relating to decision-making procedures that contain data to be ambivalent. In the year of 1943, Warren McCulloch and Walter Pitts developed NNs, representing the motivation from the brain neurons' operation. The "connectionism," includes the usage of connected neurons. Subsequently, ANFIS can be extensively employed in research to imitate global problem. In the year of 1993, Jang et al. designed a hybrid NN called ANFIS by integrating the FL and NNs. ANFIS can have 2 inputs and one output with 5 layer. By using the sigmoid membership functions, the inputs could be adapted into fuzzy inputs. This given one will be a mathematical formula for producing fuzzy inputs in layer 1:

$$O_j^{l_1} = \mu_{A_j}(y_1), j = 1,2 \tag{11}$$

Now, we get,

$$Sigmoid\ \left(y_j, a, c\right) = \mu\left(y_j\right) = \frac{1}{1 + e^{-a(y_j - c)}}\ j = 1,2,3, \ldots \tag{12}$$

In layer 2, the resultant can be calculated by multiplying the received signal. The value of w_j defines the multiplication of the membership rates, as specified by using Eq. (13).

DOI: https://doi.org/10.54216/IJAACI.060201
Received: November 12, 2023 Revised: January 29, 2024 Accepted: June 23, 2024

$$O_j^{l_2} = w_j = \mu_{A_j}(y_1) \times \mu_{B_{j-2}}(y_2) \tag{13}$$

At layer 3, every node must be static and employ the outcome of layer 2 to find the standardized firing strong point for all the rules. The standardized outcome for the rule will be acquired through Eq. (14).

$$O_j^{l_3} = \overline{w_j} = \frac{w_j}{\sum_{j=1}^{2} w_j} \tag{14}$$

Normally, layer 4 is the defuzzification layer with adaptable nodes. The linear equation can be employed for the calculation of the output by multiplying the outcome of the previous layer as given below:

$$O_j^{l_4} = \overline{w_j} f_j = \overline{w_j}(p_j y_1 + q_j y_2 + r_j) \tag{15}$$

Fig. 2 illustrates the infrastructure of the ANFIS model.

$$O^{l_5} = \sum_j \overline{w_j}\, f_j = \frac{\sum_j w_j f_j}{\sum_j w_j} \tag{16}$$

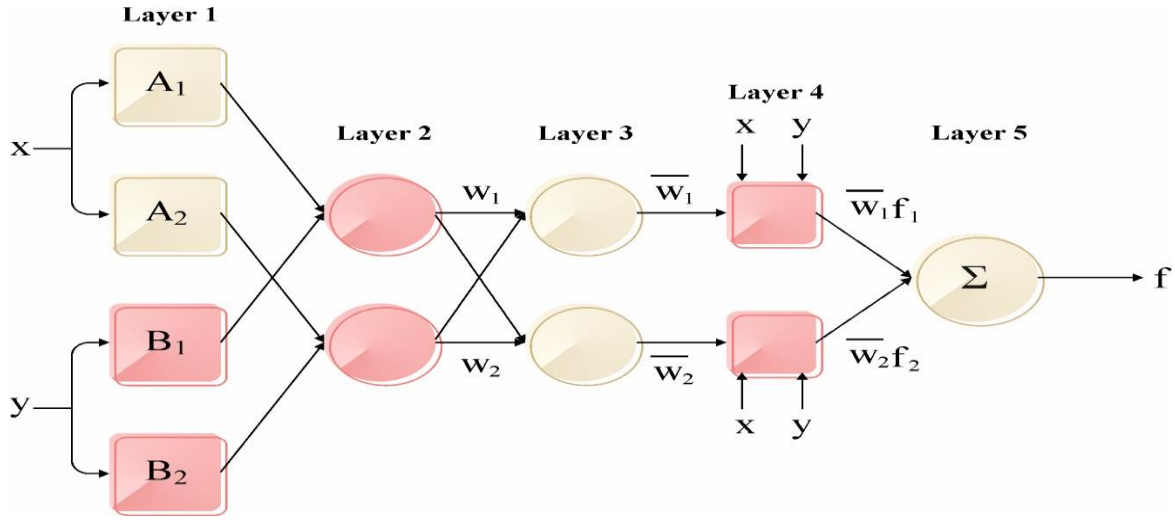

Fig. 2. Structure of ANFIS

4. Experimental Validation

This section assesses the recognition and classification performance of the HODC-TOADL technique on 2 databases: the VEDAI and the ISPRS Postdam databases. The VEDAI database contains 3687 samples with 9 classes. Besides, the ISPRS Postdam database involves 2244 samples with 4 classes. Table 1 displays the comprehensive description of two datasets.

Table 1: Details of two datasets

VEDAI database	
Classes	**No. of Instances**
Car	1340
Truck	300
Van	100
Pickup Car	950
Boat	170
Camping Car	390
Other	200

DOI: https://doi.org/10.54216/IJAACI.060201
Received: November 12, 2023 Revised: January 29, 2024 Accepted: June 23, 2024

Plane	47
Tractor	190
Total Instances	**3687**
ISPRS Postdam database	
Classes	**No. of Instances**
Car	1990
Truck	33
Van	181
Pickup Car	40
Total Instances	**2244**

Fig. 3 displays the classifier performances of the HODC-TOADL method in the VEDAI database. Figs. 3a-3b represents the confusion matrices presented by the HODC-TOADL method on 70%TRAPH:30%TESPH. The figure signified that the HODC-TOADL algorithm can be detected and categorized with 9 classes exactly. Meanwhile, Fig. 3c showcases the PR result of the HODC-TOADL approach. This experimental value defined that the HODC-TOADL method could obtain maximum PR efficiency with all classes. As well, Fig. 3d describes the ROC result of the HODC-TOADL method. This experimental value represented that the HODC-TOADL algorithm provides effective solutions with increased ROC values with 9 class labels.

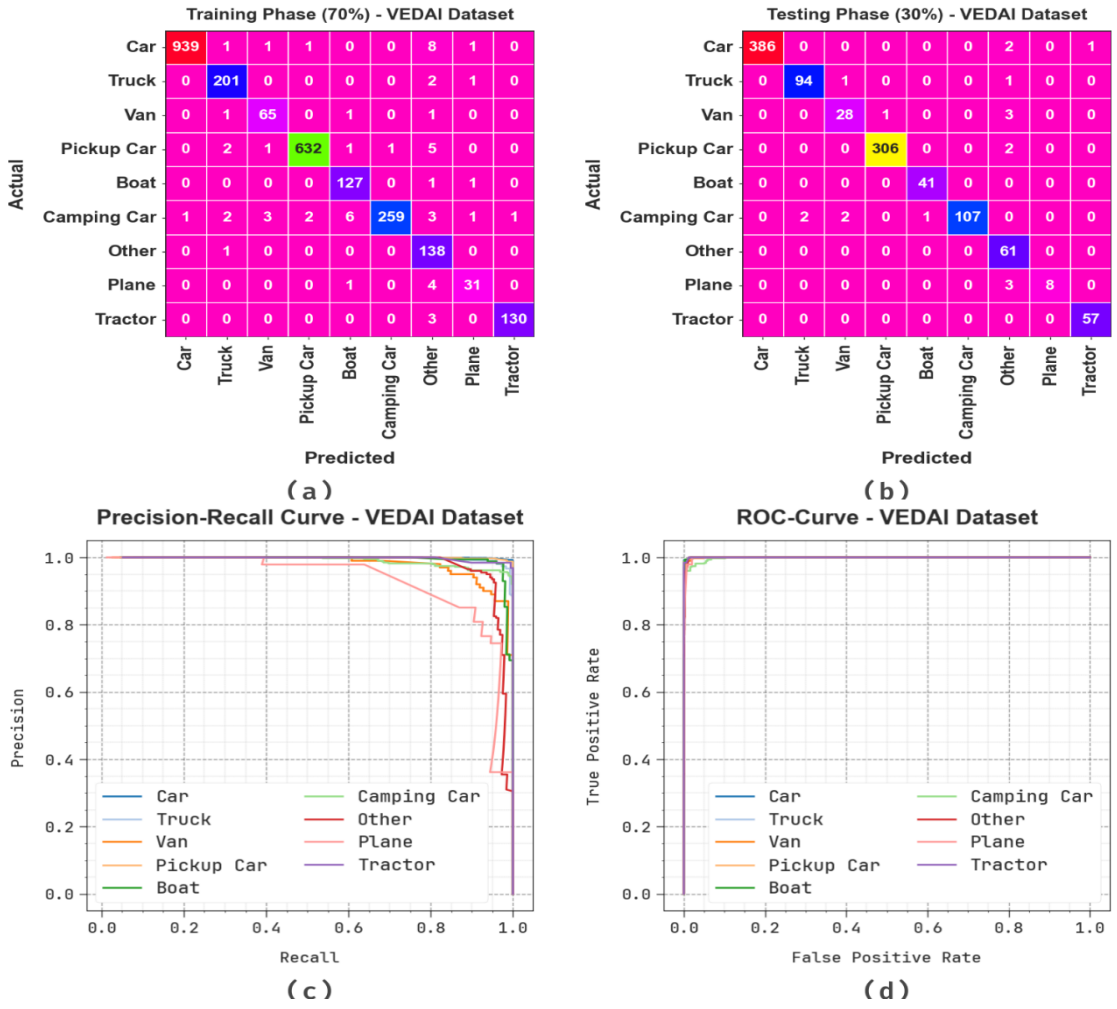

Fig. 3. VEDAI database (a-b) Confusion matrices and (c-d) PR and ROC curves

DOI: https://doi.org/10.54216/IJAACI.060201
Received: November 12, 2023 Revised: January 29, 2024 Accepted: June 23, 2024

In Table 2 and Fig. 4, the detection and classification analysis of the HODC-TOADL method are assessed on the VEDAI database. These experimentation results infer the proficient performance of the HODC-TOADL method. With 70% of TRAPH, the HODC-TOADL algorithm achieves an average $accu_y$ of 99.50%, $prec_n$ of 94.82%, $reca_l$ of 96.23%, F_{score} of 95.42%, and MCC of 95.19%. Also, with 30% of TESPH, the HODC-TOADL method gains an average $accu_y$ of 99.62%, $prec_n$ of 96.50%, $reca_l$ of 94.70%, F_{score} of 95.28%, and MCC of 95.23%.

Table 2: Classifier outcome of HODC-TOADL technique under VEDAI database

Classes	$Accu_y$	$Prec_n$	$Reca_l$	F_{Score}	MCC
TRAPH (70%)					
Car	99.50	99.89	98.74	99.31	98.92
Truck	99.61	96.63	98.53	97.57	97.37
Van	99.69	92.86	95.59	94.20	94.05
Pickup Car	99.50	99.53	98.44	98.98	98.65
Boat	99.57	93.38	98.45	95.85	95.66
Camping Car	99.22	99.62	93.17	96.28	95.92
Other	98.91	83.64	99.28	90.79	90.59
Plane	99.65	88.57	86.11	87.32	87.16
Tractor	99.84	99.24	97.74	98.48	98.41
Average	**99.50**	**94.82**	**96.23**	**95.42**	**95.19**
TESPH (30%)					
Car	99.73	100.00	99.23	99.61	99.41
Truck	99.64	97.92	97.92	97.92	97.72
Van	99.37	90.32	87.50	88.89	88.58
Pickup Car	99.73	99.67	99.35	99.51	99.32
Boat	99.91	97.62	100.00	98.80	98.76
Camping Car	99.55	100.00	95.54	97.72	97.50
Other	99.01	84.72	100.00	91.73	91.56
Plane	99.73	100.00	72.73	84.21	85.16
Tractor	99.91	98.28	100.00	99.13	99.09
Average	**99.62**	**96.50**	**94.70**	**95.28**	**95.23**

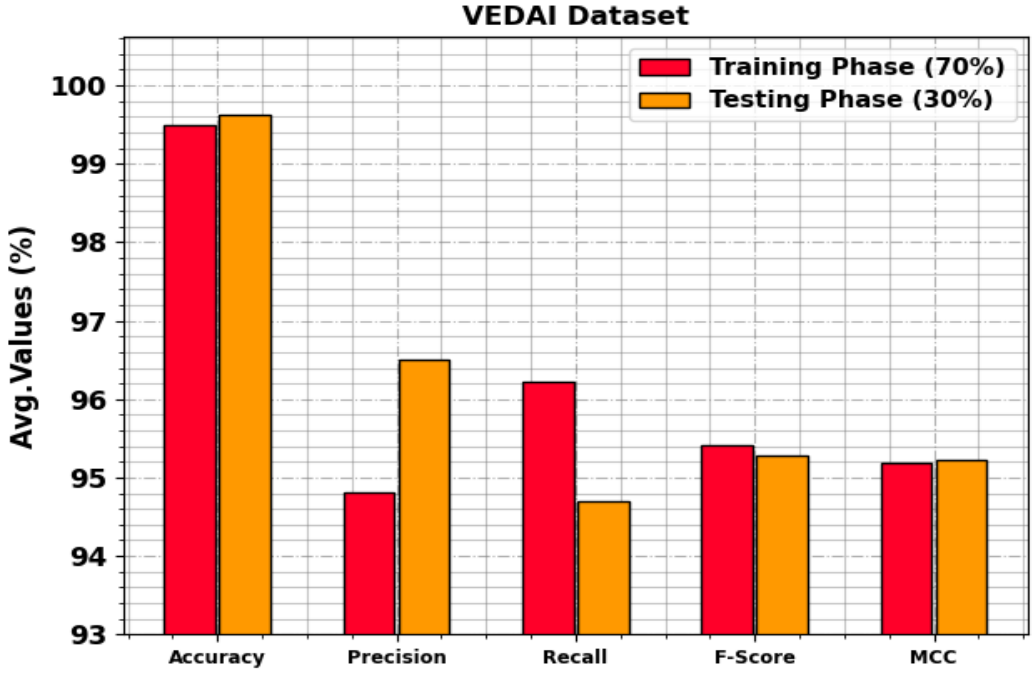

Fig. 4. Average of HODC-TOADL model under VEDAI database

DOI: https://doi.org/10.54216/IJAACI.060201
Received: November 12, 2023 Revised: January 29, 2024 Accepted: June 23, 2024

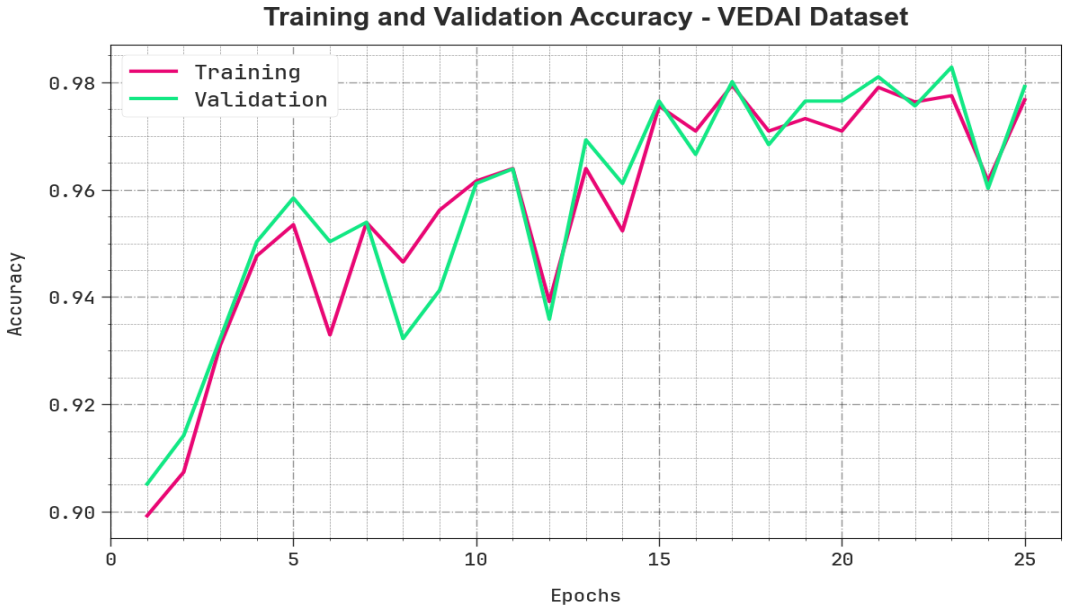

Fig. 5. $Accu_y$ Curve of HODC-TOADL model at VEDAI database

The effectiveness of the HODC-TOADL method under the VEDAI database is graphically demonstrated in Fig. 5 organized as training accuracy (TRAA) and validation accuracy (VALA) curves. This outcome shows an applied analysis of the behaviour of the HODC-TOADL model over diverse epochs, signifying its learning method and generalized abilities. Mainly, the outcome infers a constant enhancement from TRAA and VALA with development in epoch counts. It ensures that the adaptive nature of the HODC-TOADL system within the pattern detection process under both data. The increased trends in VALA outline the proficiency of the HODC-TOADL method in adapting to the TRA dataset and surpassing in giving correct classification on hidden dataset, showing the strong generalisability.

Fig. 6 illustrates a detailed review of the training loss (TRLA) and validation loss (VALL) outcomes of the HODC-TOADL technique under the VEDAI database over various epochs. The gradual decrease in TRLA emphasises the HODC-TOADL model enhancing the weights and decreasing the classifier error on both data. The outcome specifies a clear understanding of the HODC-TOADL method relevant to the TRA dataset, underlining its ability in capturing pattern. Remarkably, the HODC-TOADL method incessantly increases its parameters in reducing the differences amongst the predictive and real TRA classes.

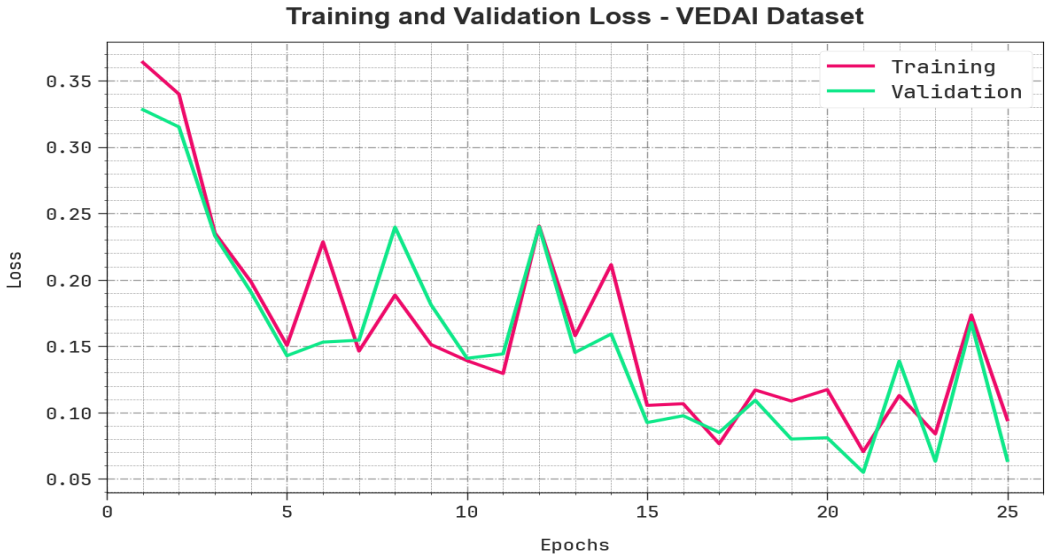

Fig. 6. Loss curve of HODC-TOADL approach under VEDAI database

DOI: https://doi.org/10.54216/IJAACI.060201
Received: November 12, 2023 Revised: January 29, 2024 Accepted: June 23, 2024

In Table 3 and Fig. 7, the HODC-TOADL method is compared with existing techniques on the VEDAI database [22]. The experimental values highlighted that LeNet and AlexNet models have reached the least $accu_y$ of 79.74% and 88.98%. At the same time, the CSOTL-VDCRS and VGG-16 models have resulted in moderate $accu_y$ values of 98.07% and 94.46%. Although the ICOA-DLVDC model has attained a considerable $accu_y$ of 99.50%, the HODC-TOADL technique ensured maximum performance with an increased $accu_y$ of 99.62%.

Table 3: $Accu_y$ result of HODC-TOADL technique with recent algorithms under VEDAI database

VEDAI database	
Methods	**Accuracy (%)**
HODC-TOADL	99.62
ICOA-DLVDC	99.50
CSOTL-VDCRS	98.07
LeNet	79.74
AlexNet	88.98
VGG16	94.46

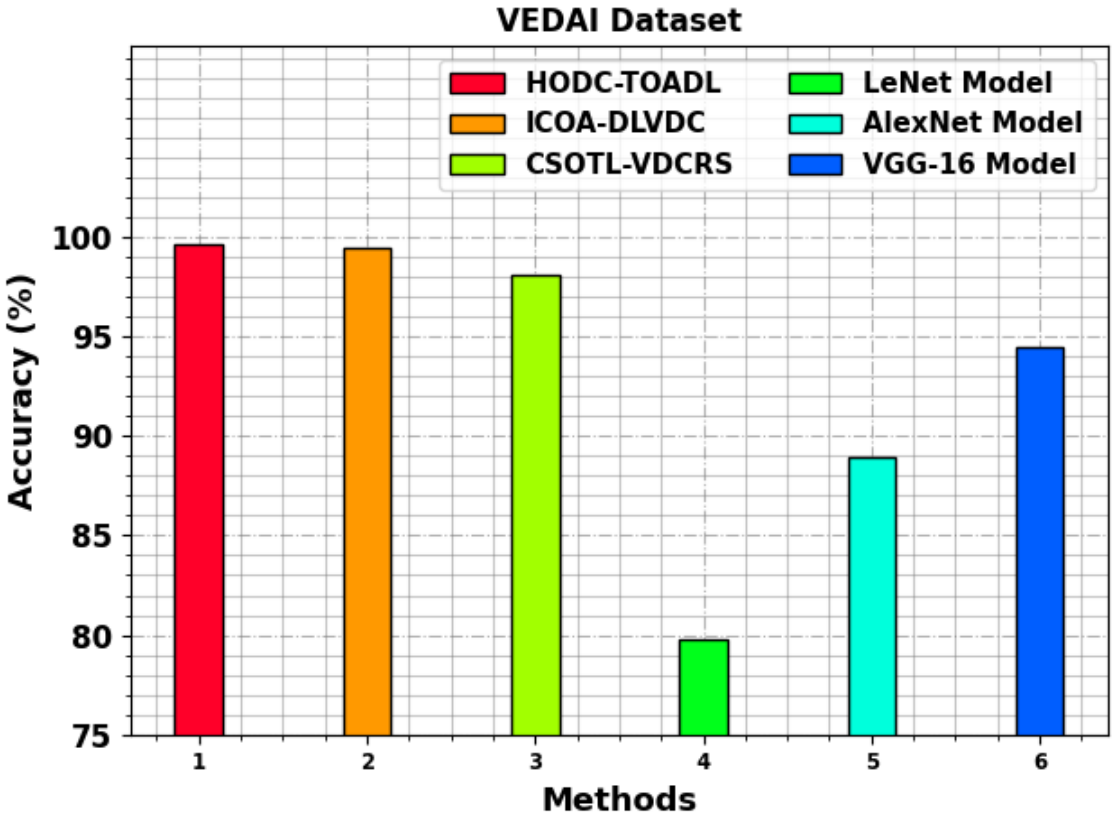

Fig. 7. $Accu_y$ Outcome of HODC-TOADL technique under VEDAI database

Fig. 8 exhibits the performance of the HODC-TOADL approach at the ISPRS Postdam database. Figs. 8a-8b describes the confusion matrices achieved by the HODC-TOADL system with 70%TRAPH: 30%TESPH. This figure indicated that the HODC-TOADL method can be detected and categorized with four classes correctly. Next, Fig. 8c reveals the PR result of the HODC-TOADL method. This figure describes that the HODC-TOADL method gains higher PR outcomes with all the classes. Briefly, Fig. 8d showcases the ROC outcome of the HODC-TOADL approach. This experimental value represented that the HODC-TOADL system offers efficient outcomes with high values of ROC with distinct classes.

DOI: https://doi.org/10.54216/IJAACI.060201
Received: November 12, 2023 Revised: January 29, 2024 Accepted: June 23, 2024

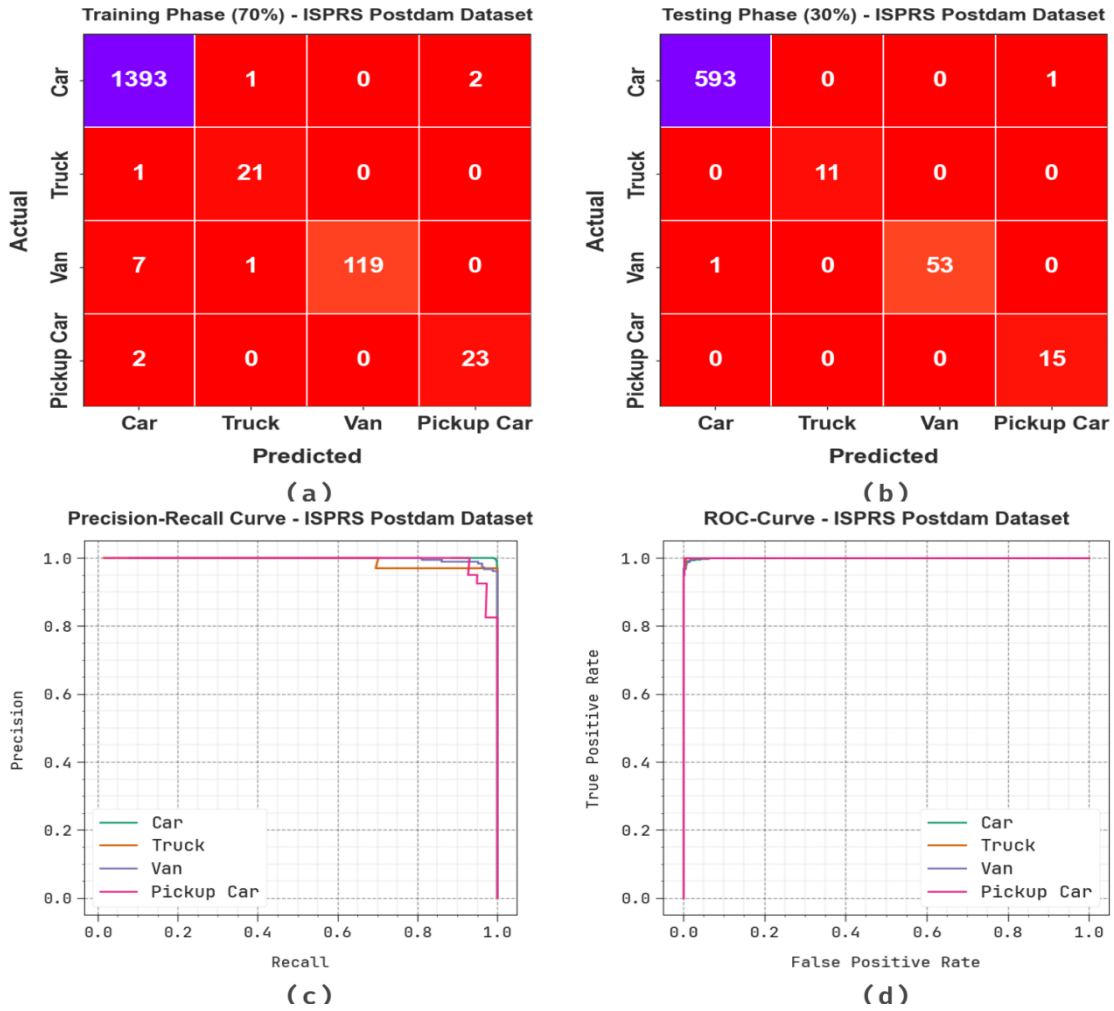

Fig. 8. ISPRS Postdam database (a-b) Confusion matrices and (c-d) PR and ROC curves

In Table 4 and Fig. 9, the detection and classification results of the HODC-TOADL approach are assessed on the ISPRS Postdam database. These experimentation outcomes denote the capable performance of the HODC-TOADL technique. According to 70% of TRAPH, the HODC-TOADL methodology gains an average $accu_y$ of 99.55%, $prec_n$ of 95.65%, $reca_l$ of 95.24%, F_{score} of 95.40%, and MCC of 94.35%. Meanwhile, based on 30% of TESPH, the HODC-TOADL algorithm gets an average $accu_y$ of 99.85%, $prec_n$ of 98.40%, $reca_l$ of 99.49%, F_{score} of 98.92%, and MCC of 98.58%.

Table 4: Classifier result of HODC-TOADL technique under ISPRS Postdam database

Classes	$Accu_y$	$Prec_n$	$Reca_l$	F_{Score}	MCC
TRAPH (70%)					
Car	99.17	99.29	99.79	99.54	95.75
Truck	99.81	91.30	95.45	93.33	93.26
Van	99.49	100.00	93.70	96.75	96.53
Pickup Car	99.75	92.00	92.00	92.00	91.87
Average	**99.55**	**95.65**	**95.24**	**95.40**	**94.35**
TESPH (30%)					
Car	99.70	99.83	99.83	99.83	98.58
Truck	100.00	100.00	100.00	100.00	100.00
Van	99.85	100.00	98.15	99.07	98.99
Pickup Car	99.85	93.75	100.00	96.77	96.75
Average	**99.85**	**98.40**	**99.49**	**98.92**	**98.58**

DOI: https://doi.org/10.54216/IJAACI.060201
Received: November 12, 2023 Revised: January 29, 2024 Accepted: June 23, 2024

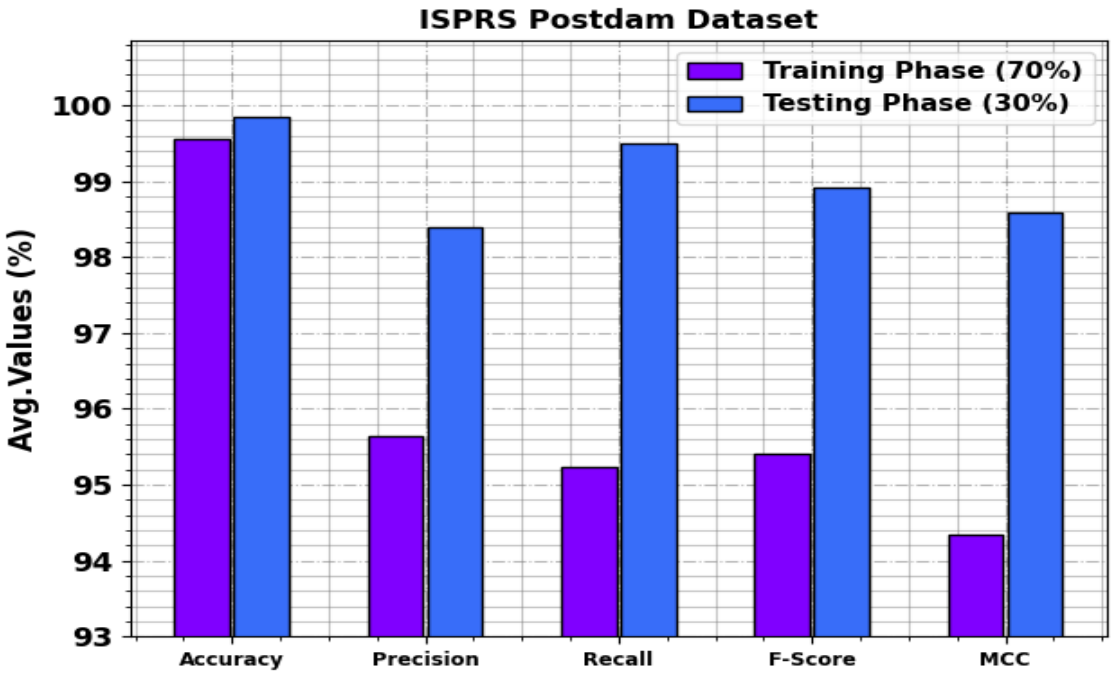

Fig. 9. Average of HODC-TOADL model on ISPRS Postdam database

The efficiency of the HODC-TOADL system under the ISPRS Postdam database is graphically presented in Fig. 10 in the procedure of TRAA and VALA curves. The outcome shown a valuable analysis of the behaviour of the HODC-TOADL methodology at some epoch count, indicating its learning method and generalized capabilities. Noticeably, the outcome denotes a consistent improvement from TRAA and VALA with evolvement in epochs. It guarantees the diverse nature of the HODC-TOADL methodology within pattern detection process under both data. The higher trends in VALA outline the ability of the HODC-TOADL algorithm to adjust to the TRA dataset and exceed in presenting accurate classifier of hidden dataset, showcasing the strong generalisabilities.

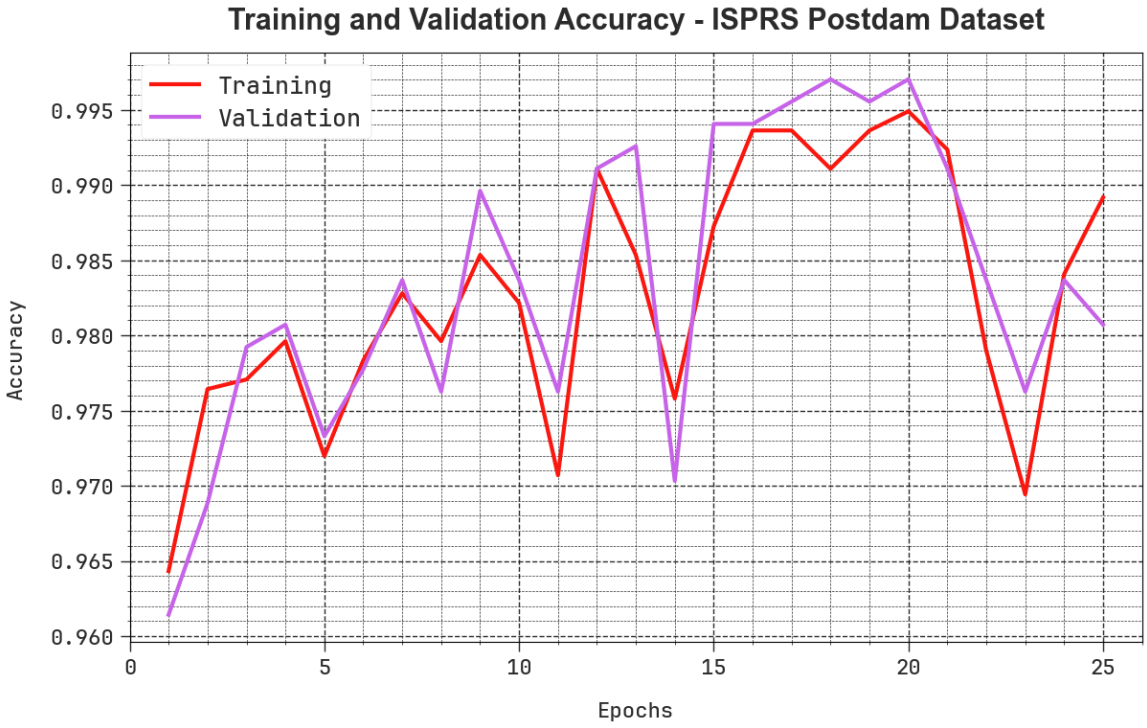

Fig. 10. $Accu_y$ Curve of HODC-TOADL method on ISPRS Postdam database

DOI: https://doi.org/10.54216/IJAACI.060201
Received: November 12, 2023 Revised: January 29, 2024 Accepted: June 23, 2024

Fig. 11 shows a detailed review of the TRLA and VALL outcomes of the HODC-TOADL method under the ISPRS Postdam database over varying epoch counts. The progressive minimizes in TRLA highpoints the HODC-TOADL method improving the weights and declining the classifier error at the both datasets. The outcome specifies a clear considerate of the HODC-TOADL technique related to the TRA dataset, emphasizing its ability in capturing patterns. Considerably, the HODC-TOADL method repeatedly increases its parameters in diminishing the variances among the predictive and real TRA classes.

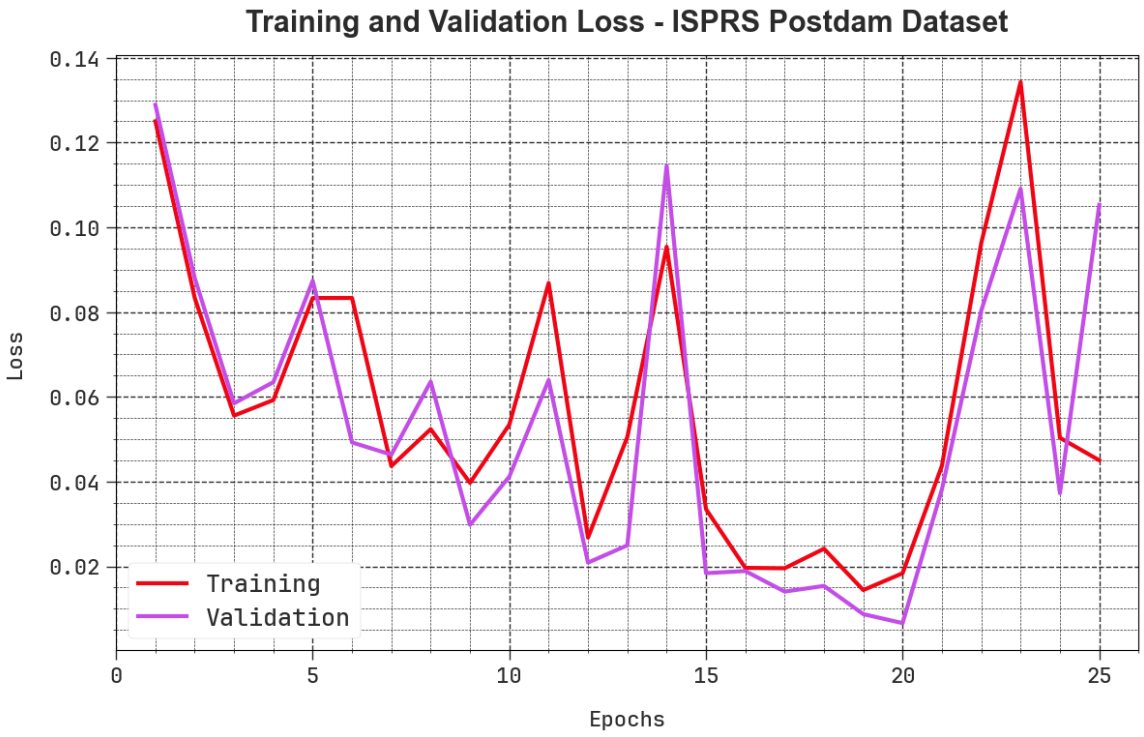

Fig. 11. Loss curve of HODC-TOADL technique under ISPRS Postdam database

Detailed outcomes of the HODC-TOADL method are compared with recent algorithms on the ISPRS Postdam database as reported in Table 5 and Fig. 12. This outcome emphasized that LeNet and AlexNet algorithms have obtained the lowest $accu_y$ of 94.54% and 95.86%. Concurrently, the CSOTL-VDCRS and VGG-16 methods have provided considerable $accu_y$ values of 98.67% and 89.54%. While the ICOA-DLVDC method has achieved considerable $accu_y$ of 99.70%, the HODC-TOADL system ensured higher performance with an improved $accu_y$ of 99.85%.

Table 5: $Accu_y$ outcome of HODC-TOADL method with existing models under ISPRS Postdam database

ISPRS Postdam database	
Methods	**Accuracy (%)**
HODC-TOADL	99.85
ICOA-DLVDC	99.70
CSOTL-VDCRS	98.67
LeNet	94.54
AlexNet	95.86
VGG-16	89.54

DOI: https://doi.org/10.54216/IJAACI.060201
Received: November 12, 2023 Revised: January 29, 2024 Accepted: June 23, 2024

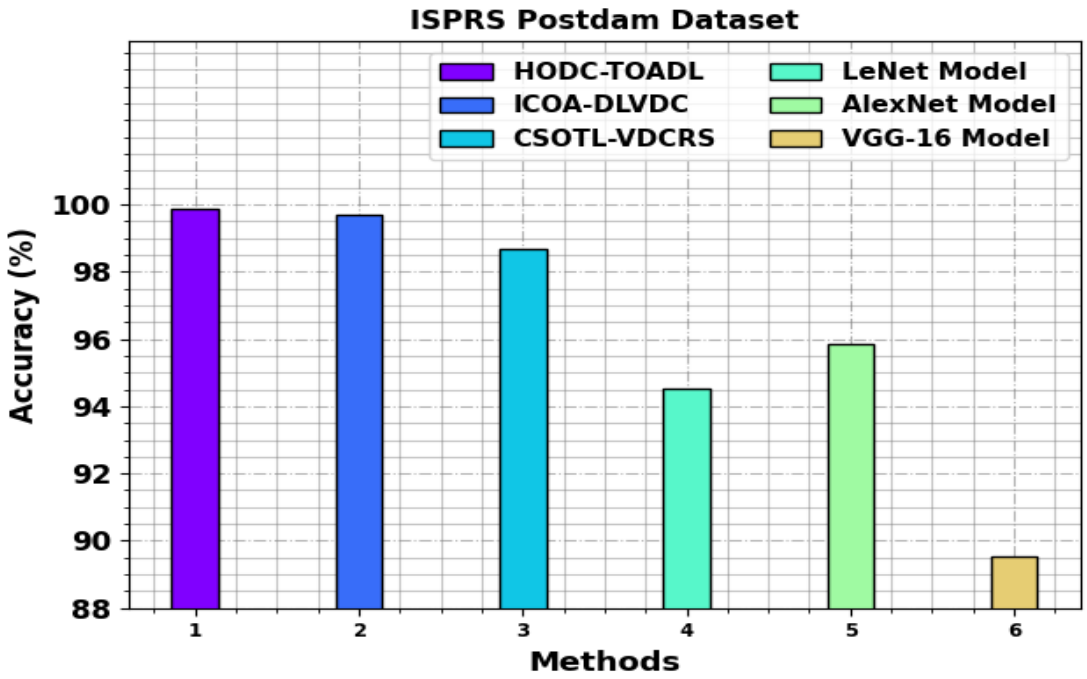

Fig. 12. $Accu_y$ Outcome of HODC-TOADL technique under ISPRS Postdam database

Therefore, the HODC-TOADL technique can be used for effectual RSI detection and classification processes.

5. Conclusion

In this study, we design an effective HODC-TOADL method. The objective of HODC-TOADL technique is to identify and classify distinct kinds of objects existing in the RSI. To attain this, the HODC-TOADL technique comprises three distinct processes including Dense Net-based feature extractor, TOA-based parameter tuning, and ANFIS-based classification. At first, the HODC-TOADL technique takes place improved Dense Net model is applied for learning the distinct features of the input RSI. Besides, the TOA can be employed to boost parameter choice of the improved Dense Net approach. Furthermore, the classification of objects can be carried out by the use of the ANFIS system. The experimental evaluation of the HODC-TOADL methodology was tested on benchmark databases. The experimental outcome stated that the HODC-TOADL algorithm reaches effective classification performance compared to recent DL models.

References

[1] Ahmed, I.; Ahmad, M.; Chehri, A.; Hassan, M.M.; Jeon, G. IoT Enabled Deep Learning Based Framework for Multiple Object Detection in Remote Sensing Images. Remote. Sens. 2022, 14, 4107.
[2] Javadi, S.; Dahl, M.; Pettersson, M.I. Vehicle Detection in Aerial Images Based on 3D Depth Maps and Deep Neural Networks. IEEE Access 2021, 9, 8381–8391.
[3] Wang, J.; Teng, X.; Li, Z.; Yu, Q.; Bian, Y.; Wei, J. VSAI: A Multi-View Dataset for Vehicle Detection in Complex Scenarios Using Aerial Images. Drones 2022, 6, 161.
[4] Safarov, F.; Temurbek, K.; Jamoljon, D.; Temur, O.; Chedjou, J.C.; Abdusalomov, A.B.; Cho, Y.I. Improved Agricultural Field Segmentation in Satellite Imagery Using TL-ResUNet Architecture. Sensors 2022, 22, 9784.
[5] Momin, M.A.; Junos, M.H.; Mohd Khairuddin, A.S.; Abu Talip, M.S. Lightweight CNN model: Automated vehicle detection in aerial images. Signal Image Video Process. 2022, 17, 1–9.
[6] Chen, Y.; Qin, R.; Zhang, G.; Albanwan, H. Spatial-temporal analysis of traffic patterns during the COVID-19 epidemic by vehicle detection using planet remote-sensing satellite images. Remote Sens. 2021, 13, 208.
[7] Wang, L.; Shoulin, Y.; Alyami, H.; Laghari, A.A.; Rashid, M.; Almotiri, J.; Alyamani, H.J.; Alturise, F. A novel deep learning—based single shot multibox detector model for object detection in optical remote sensing images. Geosci. Data J. 2022, 1–15.

DOI: https://doi.org/10.54216/IJAACI.060201
Received: November 12, 2023 Revised: January 29, 2024 Accepted: June 23, 2024

[8] Ghali, R.; Akhloufi, M.A. Deep Learning Approaches for Wildland Fires Remote Sensing: Classification, Detection, and Segmentation. Remote Sens. 2023, 15, 1821.
[9] Karnick, S.; Ghalib, M.R.; Shankar, A.; Khapre, S.; Tayubi, I.A. A novel method for vehicle detection in high-resolution aerial remote sensing images using YOLT approach. Multimed. Tools Appl. 2022, 109, 1–16.
[10] Wang, B.; Xu, B. A feature fusion deep-projection convolution neural network for vehicle detection in aerial images. PLoS ONE 2021, 16, e0250782.
[11] Zhang, M., Liu, L., Jin, Y., Lei, Z., Wang, Z. and Jiao, L., 2024. Tree-shaped multiobjective evolutionary CNN for hyperspectral image classification. Applied Soft Computing, 152, p.111176.
[12] Singh, P.S. and Karthikeyan, S., 2022. Salient object detection in hyperspectral images using deep background reconstruction based anomaly detection. Remote Sensing Letters, 13(2), pp.184-195.
[13] Mahgoub, H., Albraikan, A.A., Othman, K.M., Salama, A.S., Yaseen, I. and Ibrahim, S.S., 2023. Hyperspectral Object Detection Using Bioinspired Jellyfish Search Optimizer With Deep Learning. IEEE Access, 11, pp.126814-126822.
[14] Han, L., Tian, J., Huang, Y., He, K., Liang, Y., Hu, X., Xie, L., Yang, H. and Huang, D., 2024. Hyperspectral imaging combined with dual-channel deep learning feature fusion model for fast and non-destructive recognition of brew wheat varieties. Journal of Food Composition and Analysis, 125, p.105785.
[15] Alajmi, M., Mengash, H.A., Eltahir, M.M., Assiri, M., Ibrahim, S.S. and Salama, A.S., 2023. Exploiting Hyperspectral Imaging and Optimal Deep Learning for Crop Type Detection and Classification. IEEE Access, 11, pp.124985-124995.
[16] Chhapariya, K., Buddhiraju, K.M. and Kumar, A., 2022. CNN-Based Salient Object Detection on Hyperspectral Images Using Extended Morphology. IEEE Geoscience and Remote Sensing Letters, 19, pp.1-5.
[17] Zhao, Y., Zhang, Z., Bao, W., Xu, X. and Gao, Z., 2024. Hyperspectral image classification based on channel perception mechanism and hybrid deformable convolution network. Earth Science Informatics, pp.1-18.
[18] Islam, M.T., Islam, M.R., Uddin, M.P. and Ulhaq, A., 2023. A deep learning-based hyperspectral object classification approach via imbalanced training samples handling. Remote Sensing, 15(14), p.3532.
[19] Jiang, M., Feng, C., Fang, X., Huang, Q., Zhang, C. and Shi, X., 2023. Rice Disease Identification Method Based on Attention Mechanism and Deep Dense Network. Electronics, 12(3), p.508.
[20] Charchekhandra, B. (2023). Align and fusion two thermal and visual images. Pure Mathematics for Theoretical Computer Science, 1(1), 17-31.
[21] Jithendra, T., Khan, M.Z., Basha, S.S., Das, R., Divya, A., Chowdhary, C.L., Alahmadi, A. and Alahmadi, A.H., 2024. A novel QoS prediction model for web services based on an adaptive neuro-fuzzy inference system using COOT optimization. IEEE Access.
[22] Alajmi, M., Alamro, H., Al-Mutiri, F., Aljebreen, M., Othman, K.M. and Sayed, A., 2023. Exploiting Remote Sensing Imagery for Vehicle Detection and Classification Using an Artificial Intelligence Technique. Remote Sensing, 15(18), p.4600.

DOI: https://doi.org/10.54216/IJAACI.060201
Received: November 12, 2023 Revised: January 29, 2024 Accepted: June 23, 2024